An Alanine Residue in the M3-M4 Linker Lines the Glycine Binding Pocket of the *N*-Methyl-D-aspartate Receptor*

Michael W. Wood‡, Hendrika M. A. VanDongen, and Antonius M. J. VanDongen§

From the Department of Pharmacology, Duke University, Durham, North Carolina 27710

While attempting to map a central region in the M3-M4 linker of the *N*-methyl-D-aspartate receptor NR1 subunit, we found that mutation of a single position, Ala-714, greatly reduced the apparent affinity for glycine. Proximal *N*-glycosylation localized this region to the extracellular space. Glycine affinities of additional Ala-714 mutations correlated with side chain volume. Substitution of alanine 714 with cysteine did not alter glycine sensitivity, although this mutant was rapidly inhibited by dithionitrobenzoate. Glycine protected the A714C mutant from modification by dithionitrobenzoate, whereas the co-agonist L-glutamate was ineffective. These experiments place Ala-714 in the glycine binding pocket of the *N*-methyl-D-aspartate receptor, a determination not predicted by previous structural models based on bacterial periplasmic binding protein homology.

The *N*-methyl-D-aspartate (NMDA)[1] receptor is distinguished among the ionotropic glutamate receptors by several properties. The receptor possesses a unique Ca^{2+} permeability and a voltage-dependent Mg^{2+} block (1). These two features define the NMDA receptor's role in several important physiologic phenomena, including long term potentiation, neuronal development, and excitotoxicity (2). However, the functional characteristic that may most differentiate the NMDA receptor from other glutamate receptors is a requirement for the co-agonist glycine (3, 4). Occupancy of both glutamate and glycine binding sites is necessary for receptor activation, and the two sites are allosterically coupled (5, 6). The distinct glycine binding site has been suggested to play a role in regulation of NMDA receptor desensitization (7). While several residues in the amino terminus of NR1 have been demonstrated to greatly influence glycine affinity, binding is also modulated by the contributing NR2 subunits (8). Indeed, the glycine binding site is a current experimental target for therapeutic intervention in the hours immediately following ischemic stroke (9).

Despite functional differences among the glutamate receptors, several recent studies have converged upon a single topology model for the ionotropic glutamate receptor family (10–14). Speculation of alternate glutamate receptor topology was suggested by several early investigations (15–19). Several subsequent systematic studies concluded that non-NMDA glutamate receptor subunits possessed a three-transmembrane domain architecture (11, 12, 20). By generating functional *N*-linked glycosylation mutants of the NMDA NR1 subunit, we tested the hypothesized existence of a conserved hairpin pore structure similar to that found in voltage-gated K^+ channels (13), thus supporting the three-transmembrane domain model. An important consequence of the new three-transmembrane domain configuration is an extracellular location of the M3-M4 linker.

Inconsistent with the conclusion from these topology studies, however, were findings from several groups that residues in the M3-M4 linker of non-NMDA glutamate receptors could be phosphorylated (21–25). Most notably, two separate laboratories had determined that a serine residue (Ser-684) in the M3-M4 linker of GluR6 acted as a substrate for protein kinase A (PKA) (21, 22). The topology studies and the GluR6 phosphorylation data may be reconciled if two short transmembrane regions flanking the phosphorylation site are invoked (Fig. 1; see also Ref. 13). We have investigated this possibility utilizing the NR1 subunit through the introduction of both a novel PKA site and an *N*-linked glycosylation site in a region analogous to Ser-684 of GluR6. Subsequently, we have identified an alanine residue present in the glycine binding pocket of the NMDA receptor.

EXPERIMENTAL PROCEDURES

Site-directed Mutagenesis—Mutagenesis was performed using the mega-primer method as described previously (13). Mutations were subcloned into the pCR vector (Invitrogen) prior to insertion into a modified pN60 NR1 clone (26) containing an altered 5′-untranslated region (27) using the restriction enzymes *Sac*I (nucleotide 2058) and *Sph*I (nucleotide 2237) (New England Biolabs). Mutations were verified by DNA sequencing (U. S. Biochemical Corp.).

cRNA Synthesis and Oocyte Expression—Quantitative cRNA injections were performed as described (27). The construct ε-68 (mouse NR2A with the 5′-untranslated region truncated at nucleotide −68) was used with the coinjection experiments (28). Two separate transcription reactions of each cRNA were performed, and four batches of oocytes were injected (two of each transcription). In each case, five oocytes of each combination were tested 3 days after injection. Otherwise, cRNA was *in vitro* synthesized as described previously (13). All measurements were made from oocytes coinjected with robustly expressing ε constructs 2–5 days after injection (27).

Electrophysiology—Whole cell responses to agonist applications were obtained as described previously (13). Oocytes were held at −50 mV and perfused continuously with a Mg^{2+}- and Ca^{2+}-free solution containing (in mM) 100 NaCl, 5 KCl, 0.5 $BaCl_2$, and 10 HEPES, pH 7.4, 24 °C. Responses to submaximal agonist concentrations were preceded and followed by measurements at maximal concentrations to correct for any drift caused by gradual run-up of oocyte responses. Peak current responses to agonist application and accompanying voltage measurements were determined using PCLAMP hardware and software (Axon Instruments, Burlingame, CA). Dose-response curves for L-glutamate and glycine were fitted with the Hill equation with the Hill coefficient fixed at unity. Half-maximal concentrations (EC_{50}) were calculated by minimizing the sum of squared residuals calculated from the averaged responses at each concentration. Glycine-apparent affinities were

[1] The abbreviations used are: NMDA, *N*-methyl-D-aspartate; PKA, protein kinase A; DTNB, dithionitrobenzoic acid.
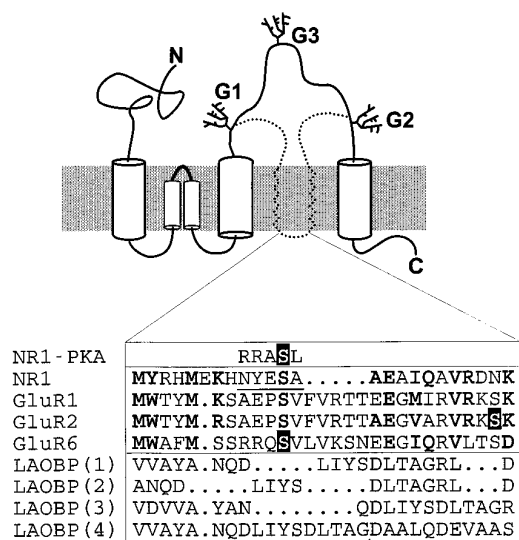
FIG. 1. **Topology and homology of ionotropic glutamate receptors..** Two functional *N*-linked glycosylation sites located at the extremes of the M3-M4 linker in the NR1 subunit (G1, P675A; G2, S773A (13)) and one located near the center of the linker (G3, this paper) are shown. The location of putative phosphorylation sites are also indicated. Beneath the topology diagram, an alignment of the NR1 sequence with several glutamate receptor subunits is shown (26, 52–55). Homologous residues appear in *boldface type*. Putative phosphorylation targets are shown with a black background: Ser-684 in GluR6 (21, 22), Ser-696 in GluR2 (25), and the artificial NR1-PKA mutation (this paper). The NR1-PKA mutation (*underlined residues* and *top row*) was constructed to encode a canonical PKA site (56–58) around an existing serine (713) using the following mutation: N710R,Y711R,E712A,A714L (710:NYESA => RRASL). The alignment also includes previous alignments of glutamate receptor subunits with LAOBP: *1*, Ref. 15; *2*, Ref. 8; *3*, Ref. 43; and *4*, Ref. 44. The *open arrow* marks the location of two amino acids (Arg and Leu) deleted from the alignment of Sutcliffe *et al.* (44) in this figure. The *closed arrow* indicates the ligand contact residue, Asp-161, of LAOBP.

measured in the presence of 100 μM L-glutamate and L-glutamate affinities in the presence of 100 μM glycine.

Western Analysis—Membranes from 30 *Xenopus* oocytes were prepared as described previously (13). Western analysis was also performed as described previously (13), except that a polyclonal antibody generated against the carboxyl terminus of NR1a (Chemicon) was employed as primary antibody because the signal produced using the monoclonal antibody generated against the M3-M4 linker of NR1 (monoclonal antibody 54.1, Pharmingen) produced a weaker signal of the G3 mutation. This may be due to disruption of the antigenic epitope by the artificial *N*-glycosylation site.

RESULTS

Introduction of a Novel PKA Site—A canonical PKA consensus sequence was designed around an existing serine in the M3-M4 linker of the NR1 subunit at a position analogous to Ser-684 of GluR6 (Fig. 1). When this mutation (NR1-PKA = 710:RRASL) was expressed in *Xenopus* oocytes in combination with the NR2A subunit, it was discovered that application of high concentrations of the co-agonist glycine were necessary to activate the receptor (Fig. 2). The apparent affinity for glycine was shifted over two orders of magnitude from that of the wild-type combination (0.5 mM *versus* 1.5 μM).

The shift in apparent affinity could have arisen from phosphorylation of the novel PKA site via basal kinase activity. To test this possibility, we reconstructed the canonical PKA sequence additionally mutating the targeted serine to alanine (Fig. 3). The mutation (NR1 710:RRAAL) did not restore the apparent affinity for the co-agonist glycine, and, in fact, produced a further rightward shift (EC$_{50}$ = 990 μM). This finding excluded the possibility that the phenotype arose from phosphorylation of the artificial site, thereby suggesting that the
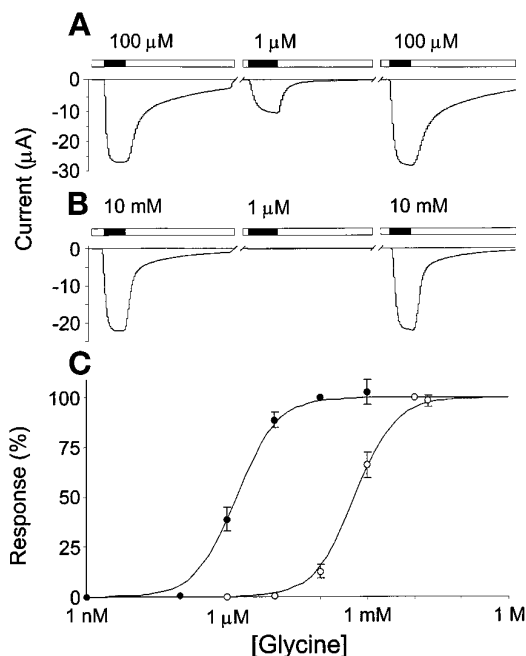

FIG. 2. **Reduced glycine sensitivity in NR1-PKA.** Responses of (*A*) wild type (NR1 + NR2A), and (*B*) mutant (NR1-PKA + NR2A) receptors expressed in *Xenopus* oocytes are shown. Responses to 100 μM L-glutamate + 1 μM glycine are shown flanked by responses to 100 μM L-glutamate + maximal glycine concentrations (100 μM and 10 mM, respectively). *Open bars above* the trace indicate perfusion of the agonist-free solution, and *filled bars* indicate agonist application. *C*, dose-response curves of the wild type (*filled circles*) and mutant (*open circles*) receptors. Mean responses are shown with standard errors of the mean (S.E.) when larger than the symbol. Calculated EC$_{50}$ values are reported in Table I.
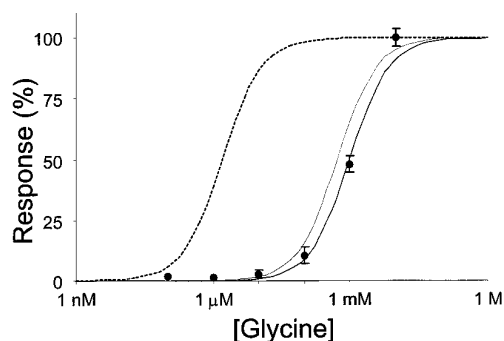

FIG. 3. **Ser-713 is not required for reduction in glycine sensitivity in NR1-PKA.** Glycine responses of the mutant receptor NR1 710:RRAAL were obtained as in Fig. 2. *Filled symbols* represent means with S.E. Curves of wild type NR1 (*dashed line*) and NR1-PKA mutant (*thin line*) receptors are redrawn from Fig. 2 for comparison.

mutated residues were interfering with glycine binding.

To identify which of the four mutated residues comprising the artificial PKA site were responsible for the shift in affinity, we generated the individual point mutants of each residue. Fig. 4*A* demonstrates that mutation of the alanine at position 714 to leucine (A714L) produced the dominant shift in glycine affinity. Furthermore, another reconstructed PKA mutation including an alanine reversion at position 714 (NR1 710:RRASA) restored most of the glycine sensitivity (EC$_{50}$ = 17 μM, see Fig. 4*B*). Therefore, position 714 is the most influential residue within the artificial PKA site affecting apparent glycine affinity. This effect may be interpreted to indicate that the presence of a leucine at position 714 interferes with ligand binding and that Ala-714 therefore is part of the glycine binding site. However, there are two problems that complicate the localization of a mutated residue to an agonist binding site: transduction and
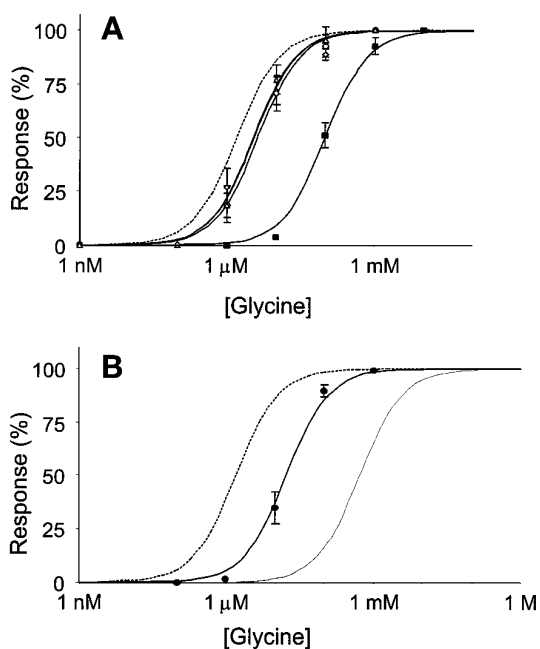
FIG. 4. **Dose-response curves of individual point mutations.** *A*, glycine dose-response curves of constructs containing the individual residues comprising the artificial PKA consensus site were obtained as shown in Fig. 2. *Symbols* represent means with S.E. as follows: N710R (*open diamonds*), Y711R (*open triangles*), E712A (*open circles*), and A714L (*filled squares*). A curve of the wild type receptor (*dashed line*) is redrawn from Fig. 2 for comparison. *B*, a dose-response curve of the point-revertant NR1 710:RRASA was constructed as in Fig. 2. *Filled symbols* represent mean with S.E. Does-response curves of wild type (*dashed line*) and NR1-PKA mutant (*thin line*) receptors are redrawn from Fig. 2.

TABLE I
Apparent affinities

Construct	Glycine	n	L-Glutamate	n
NR1	1.6	10	1.5	6
PKA	530	10		
NR1 710:RRAAL	990	7		
NR1 710:RRASA	17	7		
N710R	3.5	9	3.2	3
Y711R	3.6	7	3.4	4
E712A	4.3	7	3.8	4
A714L	100	8	0.8	4
A714C	3.0	6		
A714E	14	8		
A714F	9.7	7		
A714I	54	6		
A714K	22	7		
A714Q	54	8		
A714R	96	6		
A714T	0.4	7		
A714V	26	7		
A714Y	25	7		
Y711N,E712A (G3)	7.1	7		

propagation.

Transduction—A mutation that affects the apparent affinity of a receptor can do so by either altering ligand binding or by interfering with transduction. The transduction process encompasses all the conformational changes that follow ligand binding and that result in an increased probability for the ion channel to be open. Examples of transduction mutants are pore mutations in the nicotinic acetylcholine receptor that affected the apparent affinities for acetylcholine by (de)stabilizing the open state of the channel (29). A shift in apparent affinity alone can therefore not be used to infer localization of the mutated residue to a binding site (30).

The prospect that A714L is a transduction mutant seems less likely given the fact that the apparent affinity for the co-agonist, L-glutamate, was not concomitantly decreased in this mutant (Table I). In contrast, the mild apparent glycine and L-glutamate affinity shifts of the other three point mutants of the residues comprising the PKA consensus sequence are roughly equivalent (Table I). These mutants may disturb transduction or the allosteric coupling of the two co-agonists (5, 6).

To investigate the possibility that A714L affected transduction, we performed quantitative injection of cRNA into *Xenopus* oocytes (27). A transduction mutant that causes a rightward shift in the apparent agonist affinity would spend less time in the open state, even at maximal agonist concentrations. Such a mutant would be expected to exhibit a lower whole cell response given an equivalent receptor density. Therefore, expression levels of both heteromeric and homomeric channels measured at maximal agonist concentrations were compared (mean $\pm$ S.E., $n = 20$): NR1+NR2A 20 $\pm$ 2 μA; NR1-A714L+NR2A 26 $\pm$ 2 μA; NR1 homomer 21 $\pm$ 3 nA; NR1-A714L homomer 42 $\pm$ 8 nA. Two-tailed Student's t tests could not detect a significance difference ($p > 0.2$ for both hetero-

meric and homomeric comparisons).

Propagation—A second long-standing challenge to interpreting mutagenesis data has been to exclude the possibility that a mutation exerts its effect by introducing a structural defect which propagates to induce a conformational change in a remote part of the protein structure. It is possible that the change in apparent affinity ensuing from mutation of Ala-714 was the result of altered protein structure. In this case, modification of a distant residue could have induced a change in binding site affinity. The remaining experiments were designed to address this question.

We generated a mutation complementary to NR1-PKA, in which the targeted serine residue was incorporated into an *N*-linked glycosylation consensus site (13). Western analysis indicated that this mutant, NR1-G3, produced an increase in apparent molecular weight consistent with extracellular localization (Fig. 5). Its disruption of glycine affinity is approximately equal to a combination of point mutations at the individual residues that comprise it (Y711N,E712A *versus* Y711R and E712A, respectively, Table I). It is surprising that the attachment of a large carbohydrate moiety three amino acids upstream from position 714 does not impart a greater disturbance. This outcome suggests that position 711 already exists at the surface of the protein and that the attachment of a carbohydrate does not greatly distort the local protein structure.

Filling the Pocket—Given that an alanine side chain is an unlikely candidate for direct participation in binding glycine, we generated another series of mutations at position 714. Ten additional mutations were examined for correlation between the resulting affinities and the properties of the substituted amino acids. Of the parameters investigated (including alpha-helix and beta-strand propensity, hydrophobicity, and frequency of occurrence in defined protein structures), the only positive correlate to glycine affinity identified was side chain volume. A linear regression was performed, and the final regression model is shown in Fig. 6.

The correlation between side chain volume and affinity implies that the natural alanine residue at this position plays the architectural role of generating space for the ligand glycine. It furthermore infers that voluminous substitutions at this position create a steric hindrance that inhibits binding. Amino acids not well fit by the volume regression model may offer additional clues. Notably, the threonine mutation is the least well fit by this model. The increase in glycine affinity of the A714T mutation could be explained if the hydroxyl group of the
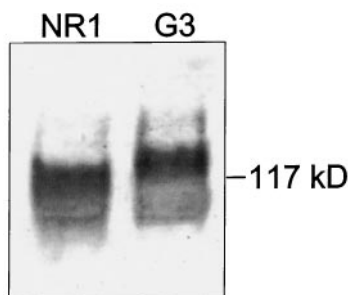
FIG. 5. **Functional *N*-glycosylation site proximal to the artificial PKA site.** An *N*-linked glycosylation consensus sequence was introduced into NR1 utilizing the endogenous target serine of the artificial PKA site (Y711N,E712A). The increases in apparent molecular weight of this mutant (NR1-G3) over that of NR1 indicates utilization of the site and thereby the extracellular location of this region of the protein.
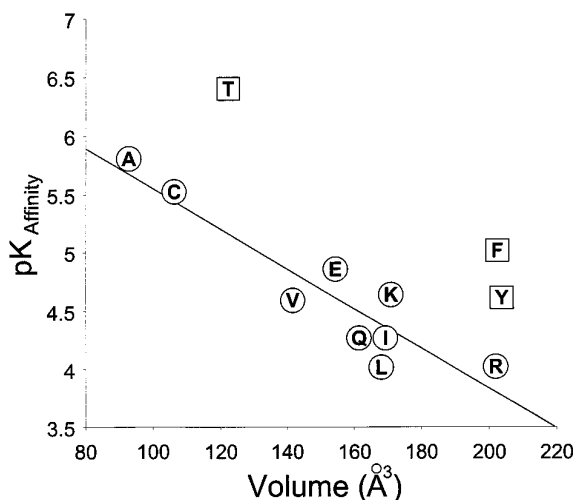

FIG. 6. **Correlation of side chain volume with glycine affinity.** Position 714 was mutated to an additional ten amino acids. A linear regression was performed using the negative log transformations of the resulting apparent affinities and the amino acid side chain volumes (59). Amino acids are represented by their single letter codes; *circled residues* are included in the final regression model, and residues enclosed in *squares* were identified as outliers. The final regression model is represented with a *line*. Analysis of variance (ANOVA) of all data points yielded a *p* value < 0.01. Studentized deleted residual analysis identified A714T and A714F as outliers ($p < 0.05$ and $p < 0.10$, respectively). Refinement of the regression model by excluding these residues decreased the ANOVA *p* value to less than 0.005 and subsequently identified A714Y as the next most influential outlier ($p < 0.15$). Removal of this second aromatic residue resulted in the final regression model (ANOVA $p < 0.0001$, correlation coefficient $r = 92\%$).

threonine was capable of substituting for a water molecule otherwise neighboring the glycine molecule. Along these lines, it is interesting to note that the volume correlation neatly divides the hydrophilic amino acids from the more hydrophobic. The two aromatic residues also impart less disturbance than their volumes would predict. This may be a product of their unique geometry or the particular affinity that glycine possesses for aromatics (8).

An alternate explanation of volume correlation would propose that larger amino acids exhibit greater disruption of proper protein folding and that the consequence of this disruption is decreased glycine affinity. The A714C mutation presented an opportunity to test this alternate interpretation. Cysteine is similar in size to alanine, and the A714C mutation exhibits a glycine affinity similar to that of the wild type receptor (Table I). Therefore, it can be assumed that little disruption of protein folding is generated by the A714C mutation. We utilized the unique reactivity of the cysteine residue to
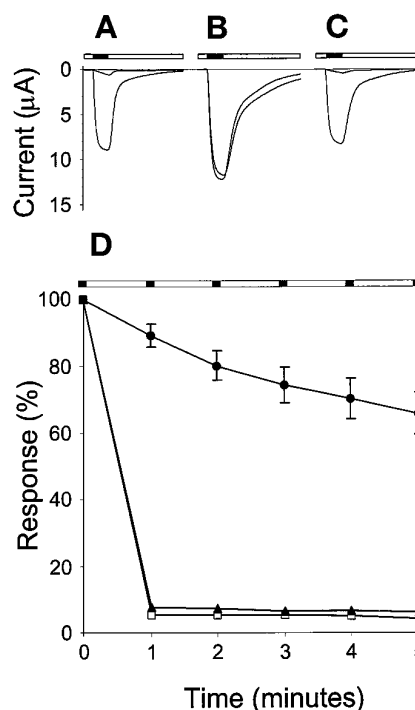

FIG. 7. **Inhibition of A714C by DTNB is protected by glycine.** *A–C*, representative traces of the A714C mutation before and after a 1-min exposure to 500 μM DTNB. *Open bars above* the trace indicate perfusion of the DTNB solution, and *filled bars* indicate DTNB-free agonist application (100 μM L-glutamate + 100 μM glycine). Responses before and after exposure to DTNB (*A*), DTNB coapplied with 100 μM glycine (*B*), and DTNB coapplied with 100 μM L-glutamate (*C*) are shown. *D*, time course of inhibition by DTNB and protection by glycine. The time course of DTNB inhibition is represented by *open squares* (*A*), the protection by 100 μM glycine by *filled circles* (*B*), and the lack of protection by 100 μM L-glutamate by *filled triangles* (*C*). All agonist response measurements and DTNB applications were performed at pH 8.0 to increase selectivity for free thiols (31). Responses of the wild type receptor are omitted for clarity. No inhibition of the wild type receptor by DTNB was evident when measurements were made at pH 8.0. However, DTNB did inhibit wild type agonist responses performed at pH 7.4 in accordance with previous reports (40, 60); a 2-min exposure to 500 μM DTNB inhibited the wild type receptor 70 ± 6% (mean ± S.E., $n = 3$).

demonstrate the importance of position 714 in NMDA receptor function (Fig. 7).

Application of the thiol selective reagent dithionitrobenzoic acid (DTNB) to the A714C mutation greatly inhibited the function of the receptor (95% inhibition in 1 min). This oxidizing agent forms a mixed disulfide with free thiols. The mixed disulfide may remain or proceed to formation of a cysteine-cysteine bond in some instances (31, 32). Because of a slow reversibility of the inhibition incurred by A714C upon DTNB exposure, we were not able to accurately assess the glycine affinity of the DTNB-labeled mutant. The reversibility may be a result of thiol-disulfide interchange (33, 34).

DTNB was therefore applied in the presence of either L-glutamate or glycine. Protection from DTNB inhibition was afforded by glycine in a time-dependent manner. Co-application of L-glutamate, however, did not protect from DTNB inhibition. Selective protection by glycine but not L-glutamate argues against the possibility that the changes in glycine affinity arise from global changes in protein folding. Rather, it suggests that the presence of glycine protects A714C from reaction with DTNB by limiting the access of DTNB to the glycine binding pocket of the NMDA receptor. Probing of a ligand binding site with cysteine substitutions has been performed previously (35, 36). Limited protection from a cysteine labeling reaction has also been demonstrated (35). However, this experiment offers a

unique view of the time course of protection by the endogenous agonist from the reaction of a residue in a ligand binding site.

DISCUSSION

Our previous results indicated that both extremes of the M3-M4 linker of the NMDA receptor NR1 subunit exist in the extracellular space. This supported the hypothesized existence of a conserved hairpin pore structure similar to that found in voltage-gated K^+ channels (13, 37). Subsequent evidence suggests that four other sites of the M3-M4 linker of NR1 are extracellular (14). In our current study, three separate measures provide further support to the three-transmembrane domain model. The shifts in glycine affinity, the increase in apparent molecular weight of an *N*-linked glycosylation site, and the unique susceptibility of a cysteine residue, each arising from mutations in the central portion of the M3-M4 linker, are all consistent with extracellular localization.

The significance of the M3-M4 linker in ionotropic glutamate receptor function has been recognized in a number of previous investigations (38–42). In fact, a segment of the M3-M4 linker has been assigned as the second of two lobes (S1 and S2) required for agonist binding, based on the homology between glutamate receptors and bacterial periplasmic binding proteins (8, 14, 15, 43–45). An important consequence of our findings is that the designation of position 714 as part of the glycine binding pocket is not predicted by the recognized homology between glutamate receptors and the bacterial periplasmic binding proteins (Fig. 1).

This homology was used as a framework for the mutagenesis study that first revealed a contribution of the M3-M4 linker of the NMDA receptor to apparent glycine affinity (8). The authors superimposed the NR1 sequence onto the known three-dimensional structure of a member of the class of bacterial proteins (the lysine/arginine/ornithine binding protein or LAOBP) to generate a structural model of the glycine binding site of the NMDA receptor. The model was recently refined when several other residues in the M3-M4 linker were identified that affect apparent glycine affinity (14).

A detailed three-dimensional prediction of the structure of the glutamate binding site of non-NMDA receptors was recently produced (44). This model was also based upon the known LAOBP structure. Hence, the same bacterial periplasmic binding protein homology has been used to make structural predictions about L-glutamate binding in non-NMDA receptors (15, 43–45) and glycine binding in the NMDA receptor (8, 14). However, the binding site of the LAOBP protein accommodates only a single amino acid (46), while the NMDA receptor requires binding of two different amino acids for activation.

Mutations in analogous amino-terminal S1 residues affected GluR1 L-glutamate affinity and NR1 glycine affinity similarly (8, 47). Several of the NMDA receptor S1 mutations producing large changes in glycine affinity also affected L-glutamate affinity. Thus, it has been argued that this homologous binding site is conserved among all ionotropic glutamate receptors (43). Furthermore, it has been suggested that a lack of amino acid selectivity from the homologous binding region would be expected due to the nonselective nature of the bacterial proteins (43).

Several lines of evidence argue that L-glutamate and glycine do not possess the same binding domain within the NMDA receptor. Both molecules are necessary to activate the receptor (3, 4). Second, selective agonists and antagonists exist for each site (48). Finally, although the sites are allosterically coupled (5, 6), our own results and those of others (8) demonstrate that it is possible to affect the apparent affinity of one of the co-agonists without affecting the other.

There is evidence that two glycine molecules are necessary

for activation of the native NMDA receptor complex (49). Whether these ligands interact at two distinct molecular sites remains unknown. Dramatic shifts in the apparent affinity for glycine have been produced by mutations in the S1 segment of the NMDA receptor (8, 50). The influence that position 714 exerts on glycine affinity may involve a second binding site or it may arise from interactions between the S1 and S2 segments.

It is curious to note the lack of influence on glycine affinity imparted by amino acid charge at this position (see Fig. 6). Therefore, it is likely that position 714 does not directly contribute a contact point for glycine binding. Rather, the volume correlation suggests that large amino acids at position 714 obstruct the access of the ligand to its binding site through steric hindrance. Alternatively, Ala-714 could reside in a region that undergoes a conformational change following glycine binding. If the NMDA receptor undergoes a hinge-bending motion upon ligand binding similar to that proposed for the bacterial periplasmic binding proteins (46), then a large portion of the protein could become protected when the two lobes close. Such a mechanism could possibly explain ligand-induced protection from DTNB modification. However, it seems unlikely that such large-scale conformational changes are associated with binding of glycine, in the absence of L-glutamate, since this fails to activate the receptor. Because DTNB modification of A714C is protected by glycine but not L-glutamate, the alternative model would infer separate conformational alterations upon the binding of each agonist.

Position 714 occurs in a region that does not possess homology with the bacterial proteins. The failure to consistently align this region of the glutamate receptor subunits with LAOBP is evidence for the lack of homology (Fig. 1). Furthermore, neither of the structural models of the NMDA receptor predicts any proximity of position 714 to the glycine binding site (8, 14). Recently, mutation of another amino acid in the M3-M4 of the NR1 subunit has been found to impart large shifts in gycine affinity (51). This residue is not predicted to contribute to glycine binding by the structural models either. These structural models offer insufficient detail to identify the precise location of Ala-714. Inspection of the diagram in Fig. 4 of Hirai *et al.* (14) suggests, however, that position 714 is located in a beta-sheet domain quite removed from the predicted glycine contact points.

Our results define position 714 as part of the glycine binding pocket. Since the region of the NMDA receptor that comprises the glycine binding pocket is distinct from the L-glutamate binding site, models based on bacterial protein homology cannot be expected to simultaneously predict both sites. Thus, although the recognized homology between ionotropic glutamate receptors and bacterial periplasmic binding proteins has contributed significantly to the current model of glutamate receptor structure, it may not serve to fully predict the complex nature of the NMDA receptor.

REFERENCES

1. Mayer, M. L., and Westbrook, G. L. (1987) *J. Physiol. (Lond.)* **394,** 501–527
2. Nakanishi, S., and Masayuki, Y. (1994) *Annu. Rev. Biophys. Biomol. Struct.* **23,** 319–348
3. Johnson, J. W., and Ascher, P. (1987) *Nature* **325,** 529–531
4. Kleckner, N., and Dingledine, R. (1988) *Science* **241,** 835–837
5. Lester, R. A. J., Tong, G., and Jahr, C. E. (1993) *J. Neurosci.* **13,** 1088–1096
6. Priestly, T., and Kemp, J. A. (1994) *Mol. Pharmacol.* **46,** 1191–1196
7. Mayer, M. L., Vyklicky, L., Jr., and Clements, J. (1989) *Nature* **338,** 425–427
8. Kuryatov, A., Laube, B., Betz, H., and Kuhse, J. (1994) *Neuron* **12,** 1291–1300
9. Koroshetz, W. J., and Moskowitz, M. A. (1996) *Trends Pharmacol. Sci.* **17,** 227–233
10. Wo, Z. G., and Oswald, R. E. (1994) *Proc. Natl. Acad. Sci. U. S. A.* **91,** 7154–7158

11. Hollmann, M., Maron, C., and Heinemann, S. F. (1994) *Neuron* **13,** 1331–1343
12. Bennett, J. A., and Dingledine, R. (1995) *Neuron* **14,** 373–384
13. Wood, M. W., VanDongen, H. M. A., and VanDongen, A. M. J. (1995) *Proc. Natl. Acad. Sci. U. S. A.* **92,** 4882–4886
14. Hirai, H., Kirsch, J., Laube, B., Betz, H., and Kuhse, J. (1996) *Proc. Natl. Acad. Sci. U. S. A.* **93,** 6031–6036
15. O'Hara, P. J., Sheppard, P. O., Thogersen, H., Venezia, D., Haldeman, B. A., McCrane, V., Houamed, K. M., Thomsen, C., Gilbert, T. L., and Mulvihill, E. R. (1993) *Neuron* **11,** 41–52
16. Molnar, E., Mcilhinney, R. A. J., Baude, A., Nusser, Z., and Somogyi, P. (1994) *J. Neurochem.* **63,** 683–693
17. Tingley, W. G., Roche, K. W., Thompson, A. K., and Huganir, R. L. (1993) *Nature* **364,** 70–73
18. Taverna, F. A., Wang, L.-Y., MacDonald, J. F., and Hampson, D. R. (1994) *J. Biol. Chem.* **269,** 14159–14164
19. Roche, K. W., Raymond, L. A., Blackstone, C., and Huganir, R. L. (1994) *J. Biol. Chem.* **269,** 11679–11682
20. Wo, Z. G., and Oswald, R. E. (1995) *J. Biol. Chem.* **270,** 2000–2009
21. Raymond, L. A., Blackstone, C. D., and Huganir, R. L. (1993) *Nature* **361,** 637–641
22. Wang, L.-Y., Taverna, F. A., Huang, X.-P., MacDonald, J. F., and Hampson, D. R. (1993) *Science* **259,** 1173–1175
23. McGlade-McCulloh, E., Yamamoto, H., Tan, S., Brickey, D., and Soderling, T. (1993) *Nature* **362,** 640–642
24. Yakel, J., Vissavajjhala, P., Derkach, V., Brickey, D., and Soderling, T. (1995) *Proc. Natl. Acad. Sci. U. S. A.* **92,** 1376–1380
25. Nakazawa, K., Mikawa, S., Hashikawa, T., and Ito, M. (1995) *Neuron* **15,** 697–709
26. Moriyoshi, K., Masu, M., Ishii, T., Shigemoto, R., Mizuno, N., and Nakanishi, S. (1991) *Nature* **354,** 31–37
27. Wood, M. W., VanDongen, H. M. A., and VanDongen, A. M. J. (1996) *J. Biol. Chem.* **271,** 8115–8120
28. Meguro, H., Mori, H., Araki, K., Kushiya, E., Kutsuwada, T., Yamazaki, M., Kumanishi, T., Arakawa, M., Sakimura, K., and Mishina, M. (1992) *Nature* **357,** 70–74
29. Akabas, M. H., Staufer, D. A., Xu, M., and Karlin, A. (1992) *Science* **258,** 307–310
30. Colquhoun, D., and Farrant, M. (1993) *Nature* **366,** 510–511
31. Habeeb, A. F. S. A. (1972) *Methods Enzymol.* **25,** 457–464
32. Faulstich, H., and Heintz, D. (1995) *Methods Enzymol.* **251,** 357–366
33. Kanarek, L., Bradshaw, R. A., and Hill, R. L. (1965) *J. Biol. Chem.* **240,** 2755–2757
34. Webster, A., Hay, R., and Kemp, G. (1993) *Cell* **72,** 97–104
35. Javitch, J., Fu, D., Chen, J., and Karlin, A. (1995) *Neuron* **14,** 825–831
36. McLaughlin, J. T., Hawrot, E., and Yellen, G. (1995) *Biochem. J.* **310,** 765–769
37. Wo, Z. G., and Oswald, R. E. (1995) *Trends Neurosci.* **18,** 161–168
38. Sommer, B., Keinänen, K., Verdoorn, T. A., Wisden, W., Burnashev, N., Herb, A., Köhler, M., Takagi, T., Sakmann, B., and Seeburg, P. H. (1990) *Science* **249,** 1580–1585
39. Sekiguchi, M., Doi, K., Zhu, W.-S., Watase, K., Yokotani, N., Wada, K., and Wenthold, R. (1994) *J. Biol. Chem.* **269,** 14559–14565
40. Sullivan, J., Traynelis, S., Chen, H., Escobar, W., Heinemann, S., and Lipton, S. (1994) *Neuron* **13,** 929–936
41. Partin, K., Bowie, D., and Mayer, M. (1995) *Neuron* **14,** 833–843
42. Kashiwagi, K., Fukuchi, J.-I., Chao, J., Igarashi, K., and Williams, K. (1996) *Mol. Pharmacol.* **49,** 1131–1141
43. Stern-Bach, Y., Bettler, B., Hartley, M., Sheppard, P. O., O'Hara, P. J., and Heinemann, S. F. (1994) *Neuron* **13,** 1345–1357
44. Sutcliffe, M., Wo, Z. G., and Oswald, R. (1996) *Biophys. J.* **70,** 1575–1589
45. Kuusinen, A., Arvola, M., and Keinanen, K. (1995) *EMBO J.* **14,** 6327–6332
46. Oh, B.-H., Pandit, J., Kang, C.-H., Nikaido, K., Gokcen, S., Ames, G. F.-L., and Kim, S.-H. (1993) *J. Biol. Chem.* **268,** 11348–11355
47. Uchino, S., Sakimura, K., Nagahari, K., and Mishina, M. (1992) *FEBS Lett.* **308,** 253–257
48. Hollmann, M., and Heinemann, S. (1994) *Annu. Rev. Neurosci.* **17,** 31–108
49. Clements, J. D., and Westbrook, G. L. (1991) *Neuron* **7,** 605–613
50. Wafford, K. A., Kathoria, M., Bain, C. J., Marshall, G., Le Bourdelles, B., Kemp, J. A., and Whiting, P. J. (1995) *Mol. Pharmacol.* **47,** 374–380
51. Williams, K., Chao, J., Kashiwagi, K., Masuko, T., and Igarashi, K. (1996) *Mol. Pharmacol.* **50,** 701–708
52. Hollmann, M., O'Shea-Greenfield, A., Rogers, S. W., and Heinemann, S. (1989) *Nature* **342,** 643–648
53. Boulter, J., Hollmann, M., O'Shea-Greenfield, A., Hartley, M., Deneris, E., Maron, C., and Heinemann, S. (1990) *Science* **249,** 1033–1037
54. Keinänen, K., Wisden, W., Sommer, B., Werner, P., Herb, A., Verdoorn, T. A., Sakmann, B., and Seeburg, P. H. (1990) *Science* **249,** 556–560
55. Egebjerg, J., Bettler, B., Hermans-Borgmeyer, I., and Heinemann, S. (1991) *Nature* **351,** 745–748
56. Feramisco, J. R., Glass, D. B., and Krebs, E. G. (1980) *J. Biol. Chem.* **255,** 4240–4245
57. Kemp, B. E. (1979) *J. Biol. Chem.* **254,** 2638–2642
58. Kemp, B. E., and Pearson, R. B. (1990) *Trends Biochem. Sci.* **15,** 342–346
59. Chothia, C. (1984) *Annu. Rev. Biochem.* **53,** 537–572
60. Kohr, G., Eckardt, S., Luddens, H., Monyer, H., and Seeburg, P. H. (1994) *Neuron* **12,** 1031–1040